# Improvement of in vitro stability and pharmacokinetics of hIFN-α by fusing the carboxyl-terminal peptide of hCG β-subunit

Natalia Ceaglio [a,*], Agustina Gugliotta [a], María Belén Tardivo [b], Dianela Cravero [a], Marina Etcheverrigaray [a], Ricardo Kratje [a], Marcos Oggero [a]

[a] Cell Culture Laboratory, School of Biochemistry and Biological Sciences, Universidad Nacional del Litoral, Ciudad Universitaria, Paraje "El Pozo", C.C. 242, S3000ZAA Santa Fe, Argentina
[b] Zelltek S.A., PTLC RN 168, S3000ZAA Santa Fe, Argentina

## ARTICLE INFO

## ABSTRACT

Improving *in vivo* half-life and *in vitro* stability of protein-based therapeutics is a current challenge for the biopharmaceutical industry. In particular, recombinant human interferon alpha-2b (rhIFN-α2b), which belongs to a group of cytokines extensively used for the treatment of viral diseases and cancers, shows a poor stability in solution and an extremely short plasma half-life which determines a strict therapeutic regimen comprising high and repeated doses. In this work, we have used a strategy based on the fusion of the carboxyl-terminal peptide (CTP) of human chorionic gonadotropin (hCG) β-subunit, bearing four O-linked oligosaccharide recognition sites, to each or both N- and C-terminal ends of rhIFN-α2b. Molecules containing from 5 (CTP-IFN and IFN-CTP) to 9 (CTP-IFN-CTP) O-glycosylation sites were efficiently expressed and secreted to CHO cells supernatants, and exhibited antiviral and antiproliferative bioactivities *in vitro*. Significant improvements in pharmacokinetics in rats were achieved through this approach, since the doubly CTP-modified IFN variant showed a 10-fold longer elimination half-life and a 19-fold decreased plasma apparent clearance compared to the wild-type cytokine. Moreover, CTP-IFN-CTP demonstrated a significant increase in *in vitro* thermal resistance and a higher stability against plasma protease inactivation, both features attributed to the stabilizing effects of the O-glycans provided by the CTP moiety. These results constitute the first report that postulates CTP as a tag for improving both the *in vitro* and *in vivo* stability of rhIFN-α2b which, in turn, would positively influence its *in vivo* bioactivity.

© 2016 Elsevier B.V. All rights reserved.

## 1. Introduction

Since their discovery in the 1950s (Isaacs and Lindenmann, 1957), interferons have gained ground in therapeutic applications. Type I interferons belong to a group of cytokines which regulate resistance to viral infections, enhance innate and acquired immune responses and modulate normal and tumour cell survival and death; such properties being the causes of their extensive use for treatment of viral diseases and cancers (Borden et al., 2007; Lin and Young, 2014).

Particularly, human interferon-α2 (hIFN-α2) was the first highly active IFN subtype to be cloned in the early 1980s, and the recombinant protein was also the first cytokine to be produced and commercialized by the pharmaceutical industry. Currently, rhIFN-α2a and rhIFN-α2b produced in bacteria are licensed drugs for treatment of chronic viral hepatitis B and C, and as antitumor agents for hairy cell leukemia, melanoma, Kaposi sarcoma, follicular lymphoma, renal cell carcinoma and chronic myelogenous leukemia, either as a monotherapy or in combination with other drugs (El-Baky and Redwan, 2015; Leader et al., 2008).

Widely successful therapeutic outcomes of rhIFN-α2 are hampered by the development of adverse side effects which alter the patientsí quality of life and often demand dose reduction or premature treatment interruption (Paul et al., 2015; Sleijfer et al., 2005). These range from normally occurring mild side effects (such as fever, myalgia and headache) to neurological toxicity, revealed as depression and suicide tendency, representing a major concern that should be carefully managed. Chronic side effects also include asthenia, weight loss and autoimmune manifestations that

* Corresponding author. Fax: +54 342 4552928.
*E-mail address:* nceaglio@fbcb.unl.edu.ar (N. Ceaglio).

can greatly limit the safety and efficacy of rhIFN-α2 treatment (Uze and Tavernier, 2015). The short half-life of the cytokine is the main driver of such complications, since high and frequent doses are required to achieve the therapeutic effect. Except in rare situations, rhIFN-α2 is administered parenterally in order to avoid proteolysis, reaching a peak level within 1 h, and quickly declining to undetectable values after 24 h post-injection (Pedder, 2003; Yuan et al., 2008). Thus, the optimization of pharmacokinetics represents a key requisite for maximizing rhIFN-α2 efficacy while reducing its harmful side effects.

The covalent conjugation of polyethylene glycol (PEG) to therapeutic proteins is the most widespread technology for extending serum half-life to reduce administration frequency (Baker, 2001; Podobnik et al., 2015; Roberts et al., 2002). Although two pegylated forms of rhIFN-α2 have been successfully introduced into the market (PEGINTRON, by Schering Plough, and PEGASYS, by Roche), there are still concerns about the immunogenicity of PEG and the possibility of generation of anti-PEG antibodies which would threaten the safety and effectiveness of treatment. Other approaches for half-life extension which have not reached clinical setting yet include Fc and albumin fusion, nanoparticle encapsulation, introduction of proteolysis-resistant mutations and incorporation of new glycosyl moieties (Ceaglio et al., 2008; Choi and Park, 2006; Elliott et al., 2003; Markert et al., 2001; Sinclair and Elliott, 2005; Subramanian et al., 2007). All of them aim to reduce the elimination mechanisms of rapidly-cleared biopharmaceuticals, such as renal clearance, receptor-mediated removal and protease degradation.

The introduction of new glycans exhibits the advantage of combining properties that influence many protein clearance pathways simultaneously. Carbohydrates increase the molecular size of glycoproteins and thus reduce the rate of glomerular filtration. Renal clearance is also delayed by repulsion between the negative charges of glycosaminoglycans situated in the glomeruli and the negative charges of protein glycans conferred by terminal sialic acids (Bocci et al., 1990; Mahmood and Green, 2005). These residues also contribute to decrease the uptake of glycoproteins from circulation by the hepatocytes by restraining the binding to hepatic asialoglycoprotein receptors that have specificity for terminal galactose or N-acetylgalactosamine residues (Morell et al., 1971). Additionally, the decreased receptor affinity of glycosylated proteins can reduce clearance by receptor-mediated endocytocis (Koury, 2003). Resistance to proteolysis can also be enhanced by glycans through masking of cleavage sites, thus reducing inactivation by endogenous serum or tissue proteases (Markert et al., 2001; Subramanian et al., 2007). Our group has previously applied a strategy to incorporate new N-linked glycans in order to improve the pharmacokinetic properties of rhIFN-α2b, rendering a molecule with four N-glycosylation sites (4N-IFN) with a 20-fold increased plasma half-life which was reflected in an enhanced therapeutic activity in mice in comparison with the non-glycosylated molecule (Ceaglio et al., 2010a; Ceaglio et al., 2008). The main challenge of this strategy is the rational selection of suitable positions for introducing new N-glycosylation sites preserving, at the same time, the functional and structural properties of the protein (Marshall et al., 2003; Samoudi et al., 2015).

An alternative approach consists in the introduction of O-glycosylation sites to a therapeutic protein. Unlike N-glycosylation, a consensus sequence for O-glycosylation has not been defined yet, although there is evidence that it occurs in regions rich in Ser, Thr and Pro, and so it is more difficult to predict (Bai et al., 2015; Rudd and Dwek, 1997; Van den Steen et al., 1998). Fusion of peptides containing O-glycosylation potential glycosylation sites to the N- or C-terminal end of proteins represents a possibility to address this issue, avoiding the extensive modification of the peptide backbone.

Regarding this last approach, a strategy based on the fusion of carboxyl-terminal peptide (CTP) of human chorionic gonadotropin (hCG) β-subunit has been successfully applied. hGC, together with pituitary gonadotropins (luteinizing hormone, LH, and follicle-stimulating hormone, FSH) and thyrotropin (TSH) constitute a family of glycoprotein hormones that are heterodimers containing a common identical α-subunit covalently bound to a β-subunit which determines the biologic specificity of each protein (Pierce and Parsons, 1981). The β-subunit of hCG is distinguished from the others because of the presence of a C-terminal extension rich in Ser and Thr, and four of these residues are responsible of the existence of O-linked glycans (Birken and Canfield, 1977). This extension is believed to play a role in maintaining the prolonged half-life of hCG compared to the other hormones (Matzuk et al., 1990). Previous studies have demonstrated that fusing the CTP to β-subunits of FSH (Fares et al., 1992) and TSH (Joshi et al., 1995), α-subunit of hCG (Furuhashi et al., 1995), human growth hormone (hGH) (Fares et al., 2010) and erythropoietin (hEPO) (Fares et al., 2007; Fares et al., 2011) did not affect assembly, secretion, receptor binding affinity, and in vitro bioactivity. Moreover, the addition of O-linked oligosaccharides by CTP fusion significantly increased the half-life and in vivo potency of such proteins.

In the present study, we evaluated the effect of fusing CTP to the N-terminal end (CTP-IFN), the C-terminal end (IFN-CTP) and both ends (CTP-IFN-CTP) of rhIFN-α2b. Therefore, IFN analogs containing 5–9 potential O-glycosylation sites were constructed and a physicochemical, biological and pharmacokinetic characterization was performed. Also, the influence of O-glycans on the stability against thermal stress and plasma protease inactivation was analyzed, comprising the first report where these properties were evaluated in order to connect the effects of CTP-derived O-glycans with the in vitro and in vivo stability of CTP-fused recombinant proteins.

## 2. Materials and methods

### 2.1. Cell culture

Chinese hamster ovary (CHO-K1) cells were grown in a mixture of Dulbecco's Modified Eagle's Medium (DMEM)/Ham's F12 1:1 (Gibco, USA) supplemented with 5% (v/v) fetal calf serum (FCS) (PAA, Austria) and 2 mM glutamine (Gibco).

Human embryonic kidney (HEK293T) cells were cultured in DMEM supplemented with 10% (v/v) FCS and 2 mM glutamine.

Madin-Darby bovine kidney (MDBK) cells were grown in Minimum Essential Medium, MEM (Gibco, USA) supplemented with 10% (v/v) FCS (growth medium). For bioassays, MEM supplemented with 2% (v/v) FCS (assay medium) was employed.

The human Daudi cell line was maintained in RPMI 1640 medium (Gibco) plus 10% (v/v) FCS.

All cells were incubated at 37 °C in humidified 5% CO$_2$.

### 2.2. Design and construction of IFN variants

Three IFN variants were designed by fusing the carboxyl-terminal peptide (CTP) of hCG β-subunit to the coding sequence of hIFN-α2b: CTP-IFN (CTP was ligated to the N-terminal end), IFN-CTP (CTP was ligated to the C-terminal end) and CTP-IFN-CTP (two CTPs were ligated to IFN, one to the N-terminal and one to the C-terminal end). Recognition sites for the restriction enzymes *Sal*I and *Xba*I were added flanking both ends of the constructs. SignalP 4.1 server (http://www.cbs.dtu.dk/services/SignalP, (Petersen et al., 2011)) was used to evaluate the effect of fusing CTP to the N-terminal end of hIFN-α2b on the native signal peptide cleavage site of the cytokine. As the native cleavage site was incor-
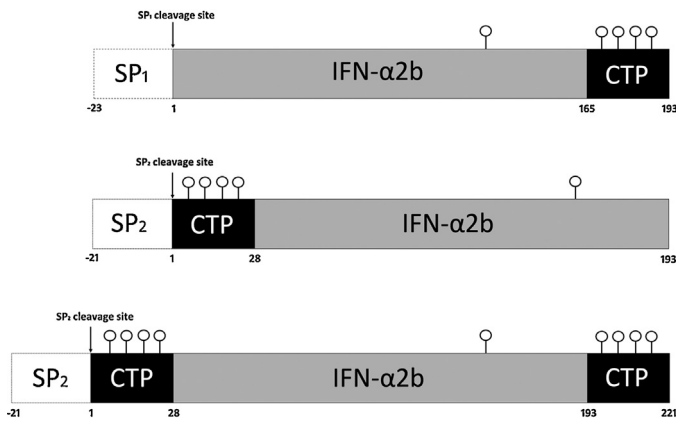
**Fig. 1.** Schematic representation of IFN-CTP, CTP-IFN and CTP-IFN-CTP constructs. Note that since fusion of CTP to the N-terminal end caused the cleavage site of hIFN-α2b signal peptide (SP$_1$) not to be correctly predicted, it was replaced by hIFN-β signal peptide (SP$_2$). Predicted O-glycosylation sites are indicated with a circle.

rectly predicted, hIFN-β signal peptide was used to ensure the secretion into the culture supernatant of IFN variants containing N-terminal end-fused CTP (Fig. 1). Probability of Ser/Thr glycosylation was estimated by employing the Isoform Specific O-glycosylation Prediction server (ISOGlyP, http://isoglyp.utep.edu/, (Leung et al., 2014)). Chimeric DNA coding for sequences of the three constructions were synthesized by GeneArt (Life Technologies, USA) and provided in cloning vectors.

### 2.3. Construction of lentiviral vectors and assembly of lentiviral particles

GeneArt plasmids were digested with SalI and XbaI and the released DNA fragments corresponding to CTP-IFN, IFN-CTP and CTP-IFN-CTP were cloned into a lentiviral plasmid (pLV). All constructs were verified by DNA sequencing.

Research grade HIV-based LV particles containing the three IFN analogs transgenes were produced following the protocol suggested by (Naldini et al., 1996) and (Dull et al., 1998). Adherent HEK293T were cultured in 10 cm-plates and simultaneously co-transfected with four plasmids: the packaging plasmid (pMDLg/pRRE) (Dull et al., 1998), the Rev-expressing plasmid (pRSV-Rev) (Naldini et al., 1996), the envelop plasmid expressing VSV-G (pMD2.G) (Dull et al., 1998), and the corresponding transfer vectors containing the transgenes (pLVs). All plasmids were introduced into the cells by liposome-mediated gene transfer, using LipofectAMINE 2000 Reagent (Invitrogen, USA), according to the supplier's instructions. Supernatants containing lentiviral particles (LVPs) were harvested 72 h post-transfection.

### 2.4. Lentiviral transduction

CHO-K1 cells were cultured on 6-well plates (Greiner, Germany) and transduced with 1 ml of supernatants containing LVPs. Twenty-four hours post-transduction, medium was replaced by fresh medium. The recombinant cell lines were subjected to a process of selective pressure using increasing concentrations of puromycin, in order to enrich the culture with the highest IFN-producing cells. Selection was started with 10 μg/ml of antibiotic, and increased until cell death or decrease of IFN productivity, which was evaluated by determination of IFN concentration by sandwich ELISA and cell counting.

### 2.5. IFN variants production and purification

The highest producing cell lines of each IFN variant were cultured for large-scale production. Cells were grown until confluence in 500 cm$^2$ triple flasks using DMEM/Hamís F12 1:1 plus 5% (v/v) FCS. The medium was then changed to basal medium supplemented with 0.5% (v/v) FCS (production medium). Every 48 or 72 h, conditioned medium was harvested and replaced with fresh production medium. Harvests were clarified by centrifugation and stored at −20 °C. Growth in triple flasks was continued for up to 20 days.

Immunoaffinity resin was prepared by coupling the anti non-glycosylated rhIFNα2b monoclonal antibody (mAb) CA5E6 (Ceaglio et al., 2008; Depetris et al., 2008) to CNBr-activated Sepharose-4B (GE Healthcare) according to the manufacturer's protocol. IFN-containing supernatants were adjusted to pH 7.5 and Triton X-100 was added to a final concentration of 0.3% (v/v). The sample was filtered through a 0.45 μm cellulose acetate membrane filter (Nalgene, USA) and applied to the immunoadsorbent column previously equilibrated with 0.3% (v/v) Triton X-100 in 25 mM Tris–HCl (pH 7,5) at a flow rate of 1 cm/min. Then, the column was washed with 5 bed volumes of the following solutions: (A) 0.5 M NaCl, 0.2% (v/v) Triton X-100 in 25 mM Tris–HCl (pH 7.5) and (B) 0.15 M NaCl. Elution of bound IFNα2b was accomplished using 0.1 M glycine (pH 2) and the pH in the eluted fractions was immediately neutralized with 1 M Tris–HCl (pH 9). Column fractions were analyzed by sandwich ELISA and those containing the higher concentrations of IFN were pooled. Purified rhIFNα2b variants were concentrated and diafiltered against ultra-pure water using Amicon Ultra-4 centrifugal filter units with 10-kDa cut-off membrane (Millipore, France). Purity was analyzed by SDS-PAGE under reducing conditions followed by Coomasie blue staining.

### 2.6. Physicochemical characterization

#### 2.6.1. Sandwich ELISA

IFN variants were quantified by a sandwich ELISA assay. In short, 96 well plates were coated overnight at 4 °C with 100 ng per well of an anti-non glycosylated rhIFNα2b mAb (Ceaglio et al., 2008; Depetris et al., 2008) in 50 mM carbonate–bicarbonate buffer (pH 9.6). After blocking 1 h at 37 °C with 1% (w/v) BSA in phosphate-buffered saline (PBS), plates were incubated with 1:2 serial dilutions of E. coli-derived rhIFNα2b standard (Gema Biotech, Argentina) from 10 ng/ml to 0.16 ng/ml or 1:2 serial dilutions of IFN analogs test samples for 1 h at 37 °C. Then, plates were incubated with an appropriately diluted rabbit anti-rhIFNα2b polyclonal antibody for 1 h at 37 °C. Finally, peroxidaselabelled goat antirabbit immunoglobulins (DAKO, Denmark) diluted 1:1,000 were added to the wells. After 1 h incubation, plates were incubated with substrate solution (0.5 mg/ml o-phenylenediamine, 0.015% (v/v) H$_2$O$_2$ in 50 mM phosphate-citrate buffer). Reaction was stopped by the addition of 2 N H$_2$SO$_4$ and the absorbance was measured at 492 nm with a microtiter plate reader (Labsystems Multiskan MCC/340, Finland). Between every step, plates were washed with PBS containing 0.05% (v/v) Tween 20 (PBS-T). Dilutions were prepared in PBS-T containing 0.1% (w/v) BSA. The assay was reproduced in duplicates.

#### 2.6.2. SDS-PAGE and western blotting

SDS-PAGE analysis was performed according to the standard method (Laemmli, 1970) using 15% (w/v) polyacrylamide resolving gels and 5% (w/v) stacking gels. Proteins were transferred onto a polyvinylidene difluoride (PVDF) membrane (Bio-Rad). Blots were blocked for 1 h with 5% (w/v) non fat milk in Tris-buffered saline (TBS) and then probed with rabbit anti-rhIFNα2b polyclonal antibodies obtained in our lab. After 1 h, blots were incubated with the same peroxidase-conjugated described in the ELISA.

Immunoreactive bands were visualized using an ECL[TM] Chemiluminescent Western Blotting Analysis System (GE Healthcare). Washes between steps were performed with TBS containing 0.05% (v/v) Tween 20 (TBS-T). Dilutions were prepared in TBS-T containing 0.5% (w/v) non fat milk.

### 2.6.3. Isoelectric focusing (IEF)

IEF was performed in 1 mm thick 8% (w/v) polyacrylamide gels containing 7 M urea, 30% (w/v) 5–7 ampholytes and 70% (w/v) 24 ampholytes. The gel was prefocused at 10 W, 2,000 V and 100 mA for 1 h. Then, 520 μl samples were applied at 1 cm from cathode and electrophoresis was carried out using the same conditions as the prefocusing step for 30 min. The IEF-separated components were detected by Coomasie blue staining.

### 2.7. In vitro IFN activity assays

#### 2.7.1. Antiviral assay

The biological antiviral activity of rhIFN-$\alpha$2b was determined by its ability to inhibit the cytopathic effect caused by vesicular stomatitits virus (VSV) on MDBK cells (Familletti et al., 1981). For this, MDBK cells were seeded into culture microtiter plates in growth medium ($2.5 \times 10^4$ cells per well) and incubated at $37\,^\circ$C overnight. After removing culture supernatants, 1:2 serial dilutions of rhIFN-$\alpha$2b WHO international standard (NIBSC 95/566) from 20 U/ml to 0.16 U/ml or 1:2 serial dilutions of rhIFN$\alpha$2b variants test samples in assay medium were added. Plates were incubated for 6 h at $37\,^\circ$C and, after removal of supernatants, an appropriate dilution of VSV virus was added. Virus replication was allowed to proceed until the cytopathic effect was clearly observable in control wells (no IFN). The medium was discarded and cells were fixed and stained simultaneously with a solution of 0.75% (w/v) crystal violet in 40% (v/v) methanol. After 10 min, plates were washed with water and the remaining dye was solubilized in 20% (v/v) acetic acid. The plates were read at 540 nm with a microtiter plate reader and the signal intensity of each dilution was reported as the mean of the absorbance measured in five wells.

#### 2.7.2. Antiproliferative assay

In order to measure rhIFN$\alpha$2b ability to inhibit cell growth, an in vitro bioassay using Daudi cells was carried out (Nederman et al., 1990). Serial 1:2 dilutions of rhIFN-$\alpha$2b WHO international standard from 100 U/ml to 0.78 U/ml or rhIFN-$\alpha$2b variants test samples were placed into microtiter plate wells. Then, previously washed Daudi cells were added ($5 \times 10^3$ cells per well) and plates were incubated at $37\,^\circ$C for 96 h. Cell proliferation was determined using a CellTiter 96[TM] AQueous Non-Radioactive Cell Proliferation Assay (Promega). Absorbance was read at 492 nm using a microplate reader. The assay was reproduced in triplicates.

### 2.8. Pharmacokinetic experiments in animals

Two-month-old female Wistar rats (Comisión Nacional de Energía Atómica, Argentina) with an average body weight of 200 g were divided into four groups of four animals each. They were housed in a temperature-controlled room at $23\,^\circ$C, with a 12 h light/dark cycle and free access to food and water. Animals were kept under identical experimental conditions except for treatment, so that a completely randomized design could be applied. Groups were injected s.c. with $1 \times 10^6$ U per body weight in a total volume of 250 μl of wildtype rhIFN$\alpha$2b (previously obtained in our lab, Ceaglio et al., 2008), CTP-IFN, IFN-CTP and CTP-IFN-CTP. Blood samples were taken at different postinjection times. Blood collected on heparin was centrifuged and plasma was stored at 20 °C. Samples were assayed for IFN antiviral activity.

All animal experimental protocols were in accordance with the "Guide for the care and use of laboratory animals" (National Research Council, USA, 2010), and efforts were made to minimize the number of animals used and their suffering.

Plots of rhIFN$\alpha$2b biological activity versus time were constructed for each animal and pharmacokinetic parameters were calculated from these plots (Shargel et al., 2005). Results were expressed as mean ± SD. Maximum plasma concentration ($C_{max}$), the time to reach the $C_{max}$ ($T_{max}$), terminal half-life ($t_{1/2}$) and apparent plasma clearance ($CL_{app}$) were calculated by the method of residuals, using Microcal Origin software version 5.0 (Microcal Software, USA). Differences between treatments were evaluated through a one-way analysis of variance (ANOVA). When the ANOVA produced significant results ($p < 0.05$), a post-hoc Tukey's multiple comparison test was applied. All statistical analyses were performed using GraphPad Prism for Windows, version 5.01 (GraphPad Software Inc.).

### 2.9. Stability assessment

#### 2.9.1. Stability against heat treatment

The thermal stability of non-glycosylated rhIFN$\alpha$2b (Gema Biotech, Argentina), wild-type IFN and CTP-IFN-CTP was investigated by determining the residual biological activity after heating at different temperatures. Samples containing 1 μg ml$^{-1}$ of the protein variants in PBS pH 7.4 were incubated in a heat block (Biometra, Germany) for 10 min at 20 °C, 25 °C, 37 °C, 45 °C, 55 °C, 65 °C, 75 °C, 85 °C and 95 °C and immediately frozen at –20 °C. Samples were assessed for IFN antiviral activity. T$m$ values (defined as the temperature at which 50% of the initial activity is lost after heat treatment) were determined from the plots of relative inactivation (%) against temperature (°C). The experiment was accomplished in duplicates.

#### 2.9.2. In vitro stability in human plasma

Purified nonglycosylated rhIFN$\alpha$2b, wild-type IFN and CTP-IFN-CTP were diluted in human plasma (obtained from healthy volunteers) to a final concentration of 50 ng ml$^{-1}$ and incubated at 37 °C. Samples were taken at different incubation times (0, 6, 24, 48, 72, 96 and 168 h) and immediately frozen at −20 °C. As the active protein concentration can be determined by measuring the biological activity of the samples, residual biological activity at different times was monitored using the antiviral assay described above.

For both stability assays, differences between molecules were evaluated through a one-way ANOVA followed by a post-hoc Tukey's test. Both statistical analyses were performed using GraphPad Prism for Windows, version 5.01. Differences between treatments were considered significant when $p < 0.05$.

### 2.10. Glycosylation analysis

#### 2.10.1. Determination of sialic acid content

Determination of sialic acid content was performed on a DIONEX ICS-5000 ion chromatography system (Thermo Scientific Dionex). 15 μg of each sample were subjected to hydrolysis with 2 M acetic acid. The released sialic acids were analysed by high-pH anion-exchange chromatography (HPAEC) using a CarboPac[TM] PA20 ($3 \times 30$ mm; Thermo Scientific Dionex) column. Detection was carried out by using pulsed amperometric detection (PAD) without requiring derivatisation. For separation, a gradient was applied using mobile phases consisting in 0.1 M sodium hydroxide (solvent A) and 0.1 M sodium hydroxide containing 0.5 M sodium acetate (solvent B). Identification and quantification of different sialic acids was accomplished by comparison with calibration curves constructed using N-acetylneuraminic (Neu5Ac) and N-glycolylneuraminic (Neu5Gc) acid standards (Calbiochem).

### 2.10.2. Monosaccharide composition

To analyze monosaccharide composition, 30 μg of glycoprotein were subjected to acid hydrolysis with 2 M trifluoroacetic acid (for neutral sugars detection including Gal, Man, Glc, and Fuc) or 6 M HCl (for amino sugars detection including GalNAc and GlcNAc) during 3 h at 100 °C. Then, reaction tubes were cooled down at room temperature, the reaction mixture was dried using Concentrator Plus (Eppendorf) and dried samples were resuspended in high purity water. Released monosaccharides were analyzed by HPAEC-PAD using a DIONEX ICS-5000 ion chromatography system equipped with a CarboPac™ PA20 column. Elution was accomplished with 12 mM NaOH followed by 200 mM NaOH to regenerate the column. Monosaccharide mix standard solutions (CM-Mono-Mix-10, Ludger) were treated like sample solutions and used for the identification and quantification of peaks deriving from glycoproteins samples.

### 2.10.3. O-Glycan structure analysis

To analyze O-glycan structures, glycoprotein samples were subjected to an alkaline β-elimination reaction by incubation with a solution of $NH_4OH$ saturated with $CO_3(NH_4)_2$ for 4 h at 60 °C. Excess of $NH_4OH$ and $CO_3(NH_4)_2$ was removed by several washings with water and subsequent evaporation. Then, samples were incubated overnight at 4 °C in acetic acid 50% v/v and again the solvent was evaporated. Glycans were then fluorescently labelled by incubation with 2-aminobenzamide (2AB) reagent (Sigma) for 2 h at 65 °C. Excess of 2AB was removed by ascending paper chromatography in acetonitrile using Whatmann 3 MM paper strips. After drying, glycans were eluted from the paper with water, filtered using 0.45 μm PDVF filters (Millex, Millipore) and evaporated. Finally, samples were resuspended in water and then diluted in 80% (v/v) acetonitrile prior to injection in a TSK-gel Amide-80 column (Tosoh Bioscience) connected to a HPLC system (Waters) equipped with a fluorescence detector module ($\lambda_{exc}$ = 330 nm, $\lambda_{em}$ = 420 nm). For separation, a gradient was applied using mobile phases consisting in 50 mM formic acid adjusted to pH 4.4 with ammonia solution (solvent A) and acetonitrile (solvent B). In order to assign the fluorescently detected peaks to their corresponding O-glycan structures, the system was calibrated using a dextran ladder (Sigma), as an external standard, which was also labelled with 2AB. The number of glucose residues in each dextran peak was plotted against the retention time of the peak to obtain a standard curve. The retention time of individual glycans was converted to glucose units (GU), and potential O-glycan structures were assigned to peaks by comparing GU values to standard values reported in the literature, including those reported for fetuin, which was run as a control (Kozak et al., 2012; Royle et al., 2002; Wopereis et al., 2006).

## 3. Results

### 3.1. CTP-fusion proteins construction and expression in transduced cells

Three IFN variants were constructed: IFN-CTP, CTP-IFN and CTP-IFN-CTP (Fig. 1). ISOGlyP software was used to evaluate the propensity for O-glycosylation in CTP-fused variants. Considering that O-GalNAc-Ts (T1–T3) are the most representative and active transferases (Steentoft et al., 2013) and also that the EVP (enhancement value product) parameter was superior to 1 (Kong et al., 2015), five O-glycosylation sites were predicted to be occupied in proteins bearing a single CTP and nine sites for CTP-IFN-CTP. One of these sites corresponded to the natural O-glycosylation site present in the wild-type rhIFN-α2b.

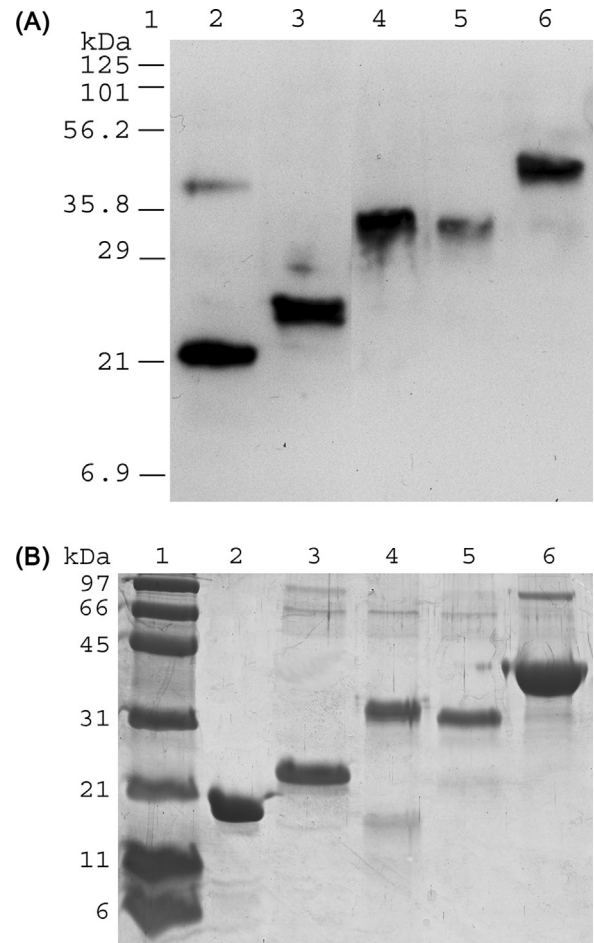Chimeric sequences were inserted into pLVs and LVPs were assembled in HEK293T cells. CHO-K1 cells were transduced with



**Fig. 2.** (A) SDS-PAGE followed by western blot of CHO-K1 derived culture supernatants containing IFN chimeras. (B) SDS-PAGE analysis followed by coomasie blue staining of immunoaffinity purified IFN variants. Lane 1, molecular mass standards; lane 2, non-glycosylated IFN; lane 3, wild-type IFN; lane 4, CTP-IFN; lane 5, IFN-CTP; lane 6, CTP-IFN-CTP.

those LVPs and stable clones with productivities of each IFN variant ranging from 0.2 μg $10^6$ $cell^{-1}$ $day^{-1}$ to 4 μg $10^6$ $cell^{-1}$ $day^{-1}$ were obtained, as assayed by sandwich ELISA. CTP moieties did not interfere with the recognition of rhIFN-α2b by the antibodies employed in the immunoassay. This was confirmed by western blot analysis under denaturing conditions using polyclonal antibodies anti-rhIFN-α2b (Fig. 2A). As demonstrated by their slower electrophoretic mobility, the three CTP-modified IFN variants exhibited a higher apparent molecular mass compared to the non-modified cytokine, thus confirming the successful incorporation of CTP and the consequent O-glycosylation. IFN chimeras containing a single CTP exhibited different electrophoretic profiles, migrating as bands corresponding to average molecular masses of 31 kDa for CTP-IFN and 29 kDa for IFN-CTP, both larger than native rhIFN-α2b (21.5 kDa). This could indicate that the position of CTP in the protein may affect the occupancy degree or the structures of the attached O-glycans, resulting in different glycosylation profiles. Fusing two CTPs to both ends of the cytokine resulted in a protein with an average electrophoretic mobility corresponding to 37 kDa, with the highest isoforms reaching 39 kDa.

### 3.2. Production, purification and characterization of chimeric IFN variants

Production of IFN variants using larger adherent cultures yielded a total accumulated mass ranging from 1.5 to 10 mg in about 20
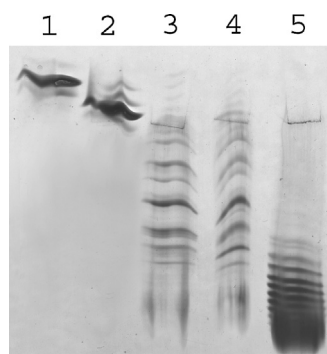
**Fig. 3.** IEF patterns of purified CTP-modified IFN analogs. Lane 1, non-glycosylated IFN; lane 2, wild-type IFN; lane 3, CTP-IFN; lane 4, IFN-CTP; lane 5, CTP-IFN-CTP.
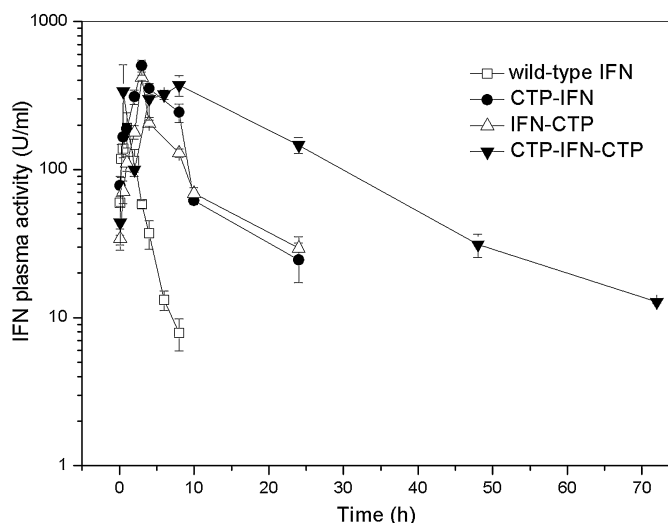


**Fig. 4.** Pharmacokinetic plasma profile of wild-type IFN, CTP-IFN, IFN-CTP and CTP-IFN-CTP dosed at $2.10^5$ U subcutaneously in Wistar rats. Data points are the average $\pm$ SEM of four animals in each group.

days. No correlation was observed between the number of CTP units and IFN variants yield.

Considering that CTP fusion to both ends of rhIFN-$\alpha$2b did not abolish the interaction of the cytokine with mAb CA5E6, a purification protocol based on immunoaffinity chromatography was employed. The three variants were captured by the immunoaffinity gel and recovered in the elution step with yields of 50–60% and high purity levels (80–85%), as judged by SDS-PAGE followed by coomasie blue staining (Fig. 2B). The molecular mass profiles of purified IFN chimeras were similar to those secreted to culture supernatants, demonstrating the absence of selective mAb binding to particular glycoforms.

The charge-based heterogeneity of CTP-fusion proteins was analyzed by IEF (Fig. 3). In accordance to literature (Kontsek, 1994), non-glycosylated *Escherichia coli*-derived rhIFN-$\alpha$2b appeared as a single band with a pI close to the upper limit of the pH gradient, while wild-type rhIFN-$\alpha$2b produced in CHO cells evidenced the presence of at least three bands corresponding to isoforms having no glycans or bearing different *O*-glycan's structures attached to residue Thr106. CTP-IFN variants exhibited a higher number of isoforms compared to the above mentioned molecules, which were distributed all along the pH separation range. Notably, the doubly modified cytokine CTP-IFN-CTP showed a wide diversity of glycoforms (more than 10 bands), with a homogeneous profile, since all of them were concentrated in the more acidic part of the pH range. These results were consistent with a higher sialic acid content conferred by the new *O*-glycosyl moieties.

Regarding *in vitro* antiviral specific biological activity, the incorporation of one CTP unit to any end of rhIFN-$\alpha$2b caused a reduction of 65–69% of the specific activity shown by the wild-type cytokine, and the addition of two CTP units led to a decrease of 75% of such activity (Table 1). *In vitro* specific antiproliferative biological activity of purified IFN variants was quite lower, retaining 6% (CTP-IFN), 8% (IFN-CTP) and 3% (CTP-IFN-CTP) of the corresponding activity of wild-type rhIFN-$\alpha$2b (Table 1). Considering that *in vitro* bioassays do not take into account pharmacokinetic differences between compounds or differences in organ distribution or metabolism (Egrie et al., 2003), the decreased *in vitro* activity of the three CTP-modified IFN variants was not an impediment to continue the characterization of the new molecules.

### 3.3. Pharmacokinetic evaluation

The influence of the CTP-derived *O*-glycans on the pharmacokinetic properties of rhIFN-$\alpha$2b was investigated after subcutaneous injection of CTP-IFN, IFN-CTP and CTP-IFN-CTP in Wistar rats. The assays were performed in comparison with the wild-type cytokine. The antiviral bioactivity profile in plasma versus time for each IFN analog is shown in Fig. 4 and the individual pharmacokinetic parameters are summarized in Table 2.

Plasma antiviral activity showed a peak at 0.8 h for wild-type IFN, 2.6 h for CTP-IFN and 2.9 h for IFN-CTP, without statistically significant differences among them. In contrast, although CTP-IFN-CTP reached a similar maximum plasma level ($C_{max}$), it was attained at 8 h post-administration, indicating an elongation of the initial distribution phase of this variant. Wild-type IFN plasma bioactivity declined rapidly and was no longer detected after 8 h, with an elimination half-life ($t_{1/2}$) of 1.4 h. Elimination phase was retarded by the addition of one unit of CTP, showing CTP-IFN and IFN-CTP a 5 to 6-fold prolonged $t_{1/2}$ compared with the wild-type protein and being detectable up to 24 h, without significant differences among them. Addition of two units of CTP drastically delayed elimination of the cytokine from circulation, since antiviral bioactivity corresponding to CTP-IFN-CTP was detected up to 72 h post-injection. This variant exhibited a $t_{1/2}$ approximately 10-fold longer than wild-type IFN and 2-fold longer than the variants carrying one CTP at any end of the protein. The exposure measured as the area under the plasma concentration curve (AUC) was considerably higher for the doubly CTP-modified variant regarding wild-type IFN and both singly CTP-modified proteins. This was directly translated into an approximately 19-fold decreased plasma apparent clearance ($CL_{app}$) for CTP-IFN-CTP in comparison with the unmodified IFN, and between 2.6 and 3.6-fold lower $CL_{app}$ regarding CTP-IFN and IFN-CTP, respectively. It is important to note that the position of CTP in IFN primary structure did not influence the pharma-

**Table 1**
*In vitro* specific bioactivities of purified CTP-IFN variants.

| rhIFN-$\alpha$2b variant | Specific antiviral bioactivity (U ng$^{-1}$) | Specific antiproliferative bioactivity (U ng$^{-1}$) |
|---|---|---|
| Wild-type IFN | $185 \pm 30$ | $309 \pm 65$ |
| CTP-IFN | $65 \pm 3$ | $19 \pm 9$ |
| IFN-CTP | $58 \pm 6$ | $26 \pm 8$ |
| CTP-IFN-CTP | $44 \pm 3$ | $9 \pm 1$ |

**Table 2**
Pharmacokinetic parameters estimated after subcutaneous administration of a single dose of CTP-IFN variants in rats.

| rhIFN-α2b variant | $T_{max}$ (h) | $C_{max}$ (U ml$^{-1}$) | $t_{1/2}$ (h) | AUC (U h ml$^{-1}$) | $Cl_{app}$ (ml h$^{-1}$) |
|---|---|---|---|---|---|
| Wild-type IFN | 0.8 ± 0.1 | 156 ± 44 | 1.4 ± 0.3 | 502 ± 165 | 427 ± 131 |
| CTP-IFN | 2.6 ± 0.2 | 297 ± 68 | 7.8 ± 0.7 | 3409 ± 514 | 60 ± 8 |
| IFN-CTP | 2.9 ± 0.7 | 184 ± 35 | 8.4 ± 1.5 | 2413 ± 58 | 83 ± 2 |
| CTP-IFN-CTP | 8.1 ± 3.3 | 296 ± 165 | 13.4 ± 1.5 | 8910 ± 2002 | 23 ± 6 |

cokinetic properties of singly CTP-modified IFN, as no significant differences were found in none of the calculated pharmacokinetic parameters ($T_{max}$, $C_{max}$, $t_{1/2}$ and $CL_{app}$). Interestingly, elimination half-life (14.6 ± 0.8 h) and $CL_{app}$ (27 ± 2 ml h$^{-1}$) of a rhIFN-α2b variant with newly introduced N-glycosylation sites, named 4N-IFN (Ceaglio et al., 2008) were quite similar to those of CTP-IFN-CTP ($t_{1/2}$ = 13.4 ± 1.5 h and $CL_{app}$ = 23 ± 6 ml h$^{-1}$).

### 3.4. Stability analysis

#### 3.4.1. Thermal stability

The most important factor affecting the stability of protein-based pharmaceuticals is temperature. Unfortunately, there is no general mechanism to describe its effect, but in most cases, the higher the temperature, the lower the protein stability (Wang, 1999). Conformational stability of a protein as measured by resistance to denaturation by heat or chaotropic agents is often considered a good first indicator of both shelf-life and in vivo half-life for therapeutic proteins. For that reason, the thermal behavior of CTP-IFN-CTP variant was compared to that of non-glycosylated IFN and wild-type IFN.

As shown in Fig. 5, all IFN variants preserved high antiviral activity values in the temperature range from 20 °C to 55 °C. However, incubation at 65 °C caused a severe drop of bioactivity of both the E. coli-derived cytokine, which demonstrated a mean T$m$ of 58.5 ± 3.9 °C, and the wild-type IFN produced in CHO cells, which contains an O-glycosylation site in Thr106 and showed a mean T$m$ of 61.9 ± 0.9 °C. No significant differences were observed between those two molecules, as we have previously found (Ceaglio et al., 2010b). In contrast, the highly O-glycosylated protein, CTP-IFN-CTP, showed a substantially increased thermal resistance, preserving more than 85% of residual activity at the higher temperature
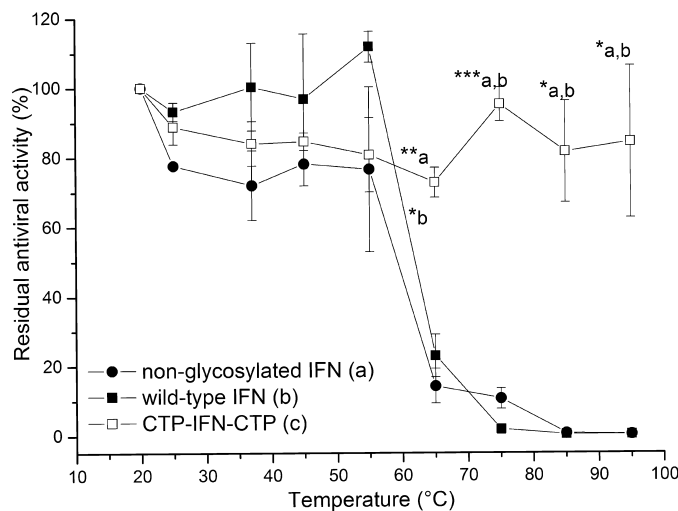
assessed (95 °C), at which the non-glycosylated and the wild-type variant showed almost no residual antiviral activity (less than 0.5% of the initial value).

#### 3.4.2. In vitro stability in human plasma

Once administered, a therapeutic protein is not only cleared from blood by glomerular filtration but it also gets exposed to another factor that affects its stability and compromises its pharmacological action: the attack of proteolytic enzymes existing in human plasma. In particular, rhIFN-α2b is rapidly inactivated by plasma proteases, constituting this mechanism one important elimination route of the cytokine from circulation (O'Kelly et al., 1985; Peleg-Shulman et al., 2004). Thus, in order to investigate if fusion of rhIFN-α2b to a peptide which confers a higher content of O-glycans would also be useful to increase its resistance to proteolytic degradation, in vitro stability of non-glycosylated IFN, wild-type IFN and CTP-IFN-CTP in the presence of human serum at 37 °C was evaluated (Fig. 6).

Under the applied conditions, antiviral bioactivity of all cytokine variants remained practically constant up to 72 h. From that time, residual bioactivity of non-glycosylated and wild-type IFN evidenced a severe drop, falling to 28% and 40% at 168 h, respectively. No significant differences were found between those two molecules. In contrast, CTP-IFN-CTP preserved intact bioactivity values (a mean of 100%) along all the time period examined, indicating that the presence of attached O-glycans may confer resistance to plasma protease inactivation. Results obtained could not be attributed to a temperature effect, since both molecules incubated at 37 °C in 0.1% (w/v) BSA in PBS showed constant (a mean of 100%) after 168 h incubation (data not shown).
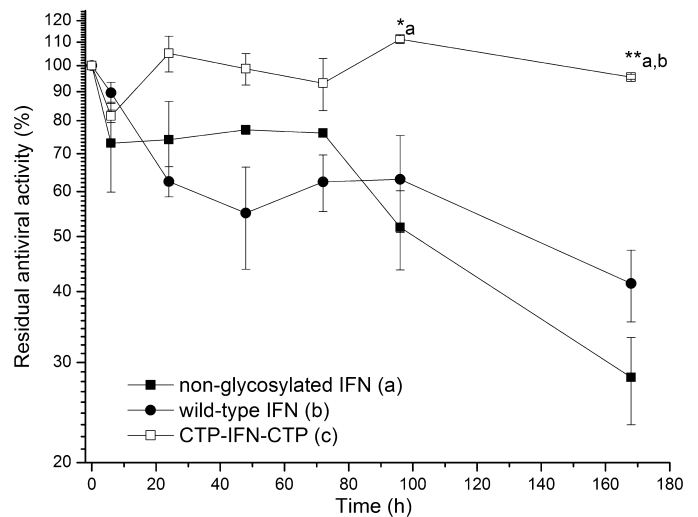


**Fig. 5.** Thermal stability of non-glycosylated IFN, wild-type IFN and CTP-IFN-CTP measured as the residual antiviral activities (%) of the IFN variants after heating at different temperatures for 10 min. Results are expressed as mean ± SEM for two independent experiments. Asterisk characters indicate significant differences between the values of a determined curve in comparison with the each of the rest of the molecules, indicated with letter a, b and c. *$p$ < 0.05; **$p$ < 0.01 and ***$p$ < 0.001.



**Fig. 6.** In vitro stability of non-glycosylated IFN, wild-type IFN and CTP-IFN-CTP in human plasma measured as the residual antiviral activity after different incubation times. Results are expressed as mean ± SEM for two independent experiments. Asterik characters indicate significant differences between the values of a determined curve in comparison with the each of the rest of the molecules, indicated with letter a, b and c. *$p$ < 0.05; **$p$ < 0.01 and ***$p$ < 0.001.
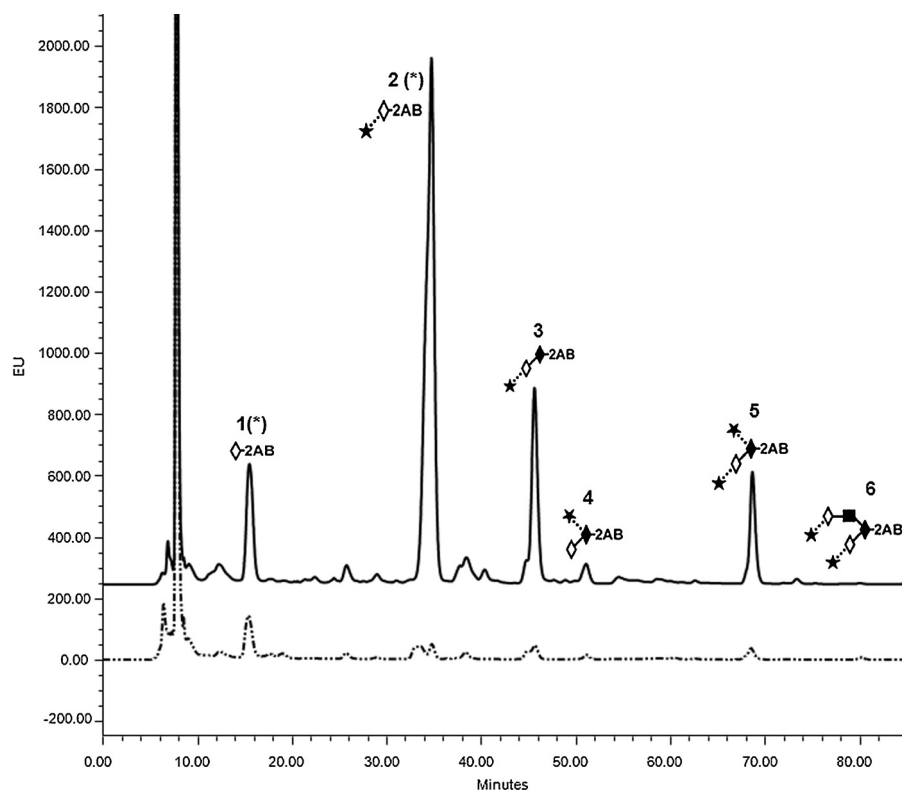
**Fig. 7.** Normal-phase HPLC profiles of 2AB-labeled *O*-linked glycans derived from CTP-IFN-CTP (—) and fetuin (- -) as reference. Probable *O*-glycan structures are indicated for major peaks. Asterisks indicate peaks resulting from peeling reactions. Symbols: ♦ GalNAc; ■ GlcNAc; ◊ Gal; ★ NeuAc.

## 3.5. O-Glycosylation characterization

### 3.5.1. Determination of sialic acid content

Sialic acid results a critical molecule to define *in vivo* bioactivity, in particular, *in vivo* half-life of a therapeutic protein. In addition, it is important to distinguish between *N*-acetylneuraminic acid (Neu5Ac) and *N*-glycolylneuraminic acid (Neu5Gc) species. The last one is present in a great variety of mammalian cells, including CHO-K1 cells, but it is not produced by human cells due to the absence of an enzyme required for its synthesis. Thus, Neu5Gc constitutes an immunogenic residue, being necessary to reduce its content in therapeutic products (Ghaderi et al., 2010; Ghaderi et al., 2012).

Average Neu5Ac content of CTP-IFN-CTP variant was found to be $8.7 \pm 0.8$ mol of sialic acid per mol of protein, while a value of $1.7 \pm 0.2$ mol of sialic acid per mol of protein was found for wild-type IFN. Minimal quantities of Neu5Gc were detected in both wild-type IFN ($0.06 \pm 0.01$ mol Neu5Gc per mol of protein) and CTP-IFN-CTP ($0.15 \pm 0.01$ mol Neu5Gc per mol of protein) samples, representing a 3.5% and 1.7% of total sialic acid species, respectively. The values of Neu5Gc obtained for CTP-IFN-CTP are within the range or even lower than those reported in the literature for other biopharmaceuticals, such as CHO-derived erythropoietin (0.13 mol Neu5Gc per mol of protein, representing 1% of total sialic acid, (Noguchi et al., 1995)), CHO-derived follitropin alfa ($\approx 0.24$ mol Neu5Gc per mol of protein, representing 2% of total sialic acid (EMA/65507/2013)) and SP2/0-derived cetuximab ($\approx 1.77$ mol Neu5Gc per mol of protein, representing 95.5% of total sialic acid, (Ghaderi et al., 2010)). This finding might indicate that fusion of *O*-glycosylated CTP to rhIFN-α2b does not modify Neu5Gc content to values that have not been reported previously for other recombinant biotherapeutic proteins.

### 3.5.2. Monosaccharide composition

Consistent with the presence of *O*-linked oligosaccharide structures, no Fuc or Man was detected in any of the samples. In general, a high content of all monosaccharides per mol of protein was found in CTP-IFN-CTP, as it was expected because of the increased number of attached *O*-glycans compared to wild-type IFN. The presence of both amino sugars GlcNAc (0.4 nmols per nmol IFN) and GalNAc (2.4 nmols per nmol IFN) in non-equal proportions suggested the existence of the two most common *O*-glycans core structures: core 1 and core 2 (Jensen et al., 2010). Considering that GlcNAc contributes to build core 2 in a proportion 1:1 GlcNAc:GalNAc but it is not present in core 1, it can be assumed that only around 0.4 mol of GalNAc of the total 2.4 mol GalNAc per mol of protein detected in CTP-IFN-CTP were derived from core 2. The amount of Gal (3 nmol per nmol IFN) was similar with what those expected for the predicted structures described above.

### 3.5.3. O-Glycan structure comparative analysis

Due to the complexity of the various carbohydrate structures, there is not a single method to efficiently analyze all of them and their study should be done by a combination of several methods. Thus, the *O*-glycan profile of CTP-IFN-CTP variant was also investigated after alkaline β-elimination under non-reducing conditions. The released oligosaccharides were labeled with the fluorophore 2-amino benzamide (2AB) and analyzed by normal-phase HPLC. Under these conditions, a "peeling" reaction occured (Royle et al., 2002) that probably resulted in peaks 1 and 2 (Fig. 7). This reaction is hard to control, and represents a concern for calculating percentages of structures, but it is still useful for identifying *O*-glycan structures attached to different proteins just for descriptive purposes.

Profiles of 2AB-labeled *O*-linked glycans from CTP-IFN-CTP and fetuin (reference) are shown in Fig. 7. Beyond "peeling"

peaks, major peaks detected for CTP-IFN-CTP corresponded to core 1 structures. The largest signal corresponded to the monosialylated NeuAcα2-3Galβ1-3GalNAc structure (peak 3), followed by a signal compatible with the bisialylated NeuAcα2-3Galβ1-3[NeuAcα2-6]GalNAc structure (peak 5). A peak of smaller area could be assigned to the monosialylated Galβ1-3[NeuAcα2-6]GalNAc isomer structure (peak 4). A very small peak which might reveal the existence of core 2 structure was detected, compatible with bisialylated NeuAcα2-3Galβ1-4GlcNAcβ1-6[NeuAcα2-3Galβ1-3]GalNAc glycans (peak 6). Also, another peak which was not found in fetuin but that has been described in literature for other glycoproteins was detected, probably attributable to the monosialylated isomers NeuAcα2-3Galβ1-4GlcNAcβ1-6[Galβ1-3]GalNAc and Galβ1-4GlcNAcβ1-6[NeuAcα2-3Galβ1-3]GalNAc. These structures account for the detection of GlcNAc residues in monosaccharide composition analysis.

## 4. Discussion

New CTP-modified IFN variants were successfully expressed by recombinant CHO cells, showing an *O*-glycosylation degree that was in agreement with the prediction analysis carried out *in silico*. Western blot analysis showed that the increase in molecular mass of CTP-modified proteins was higher than the expected from the sole addition of 28 amino acids (≈2.8 kDa), consistent with the presence of *O*-linked oligosaccharide chains in the CTP. Also, all CTP-IFN derivatives showed a higher number of isoforms compared with wild-type rhIFN-α2b in IEF analyses, confirming that *O*-glycosylation was responsible for the modification of their physicochemical properties.

The addition of CTP also accounted for the reduction of *in vitro* antiproliferative and antiviral biological activities, although none of them were blocked or impaired. This decrease may be caused by a reduction of the binding affinity for type I IFN receptor due to the increment in negative charges derived from CTP *O*-glycan's sialic acids. As it can be noted, for the three IFN variants, CTP incorporation affected antiproliferative activity to a greater extent than antiviral action. Many authors have established a relationship between the different biological activities of type I IFNs and the binding affinity to the different subunits of their cellular receptor (de Weerd et al., 2007; Kalie et al., 2008). Particularly, (Jaks et al., 2007) described that ISGF3 formation and antiviral activity correlated very well with the binding affinity towards IFNAR2, but, in contrast, the affinity towards IFNAR1, together with the stability of the ternary complex, played a key role for antiproliferative activity. (Thomas et al., 2011) demonstrated that, as a general rule, a loss of receptor binding affinity affects antiproliferative activity to a greater extent than what it does to antiviral activity. Moreover, mutations increasing binding affinity resulted in a significant increase of the antiproliferative activity, but not antiviral activity, indicating that the later requires very low doses of IFN to reach saturation, while antiproliferative activity benefits from an increased binding affinity. For example, an engineered IFN-α2 variant referred to as IFNα2(YNS), showed a modification in the electrostatic profile and a reduction of the volume of the side chains by 24 Å$^2$ as regards the wild-type cytokine (Kalie et al., 2007), showing a substantially increased *in vitro* and also *in vivo* antiproliferative activity. The authors concluded that the removal of the negatively contributing side chains increased the affinity of IFNα2(YNS) towards IFNAR1.

However, the lower *in vitro* activity of the three CTP-modified IFN variants was not discouraging, since there are numerous evidences that demonstrate the risk of relying on *in vitro* assays for predicting *in vivo* biological activity and therapeutic effects of a protein (Egrie et al., 2003). Besides, improvement of

pharmacokinetic properties is considered so vital to a protein's efficacy that many times it is achieved at the expense of its *in vitro* specific bioactivity. Examples of this behavior include the rhIFN-α2b variant with four new *N*-glycosylation sites (4N-IFN) which retains only a 10% antiviral potency and 1% antiproliferative potency compared to the corresponding ones for the wild-type cytokine. However, 4N-IFN exhibited a 10-fold longer half-life and a 20-fold decrease in systemic clearance rate compared with the unmodified protein following subcutaneous administration in rats (Ceaglio et al., 2008). More importantly, this enhanced pharmacokinetic behavior was responsible of the markedly enhanced *in vivo* antitumor activity of 4N-IFN in a model of human prostate carcinoma implanted in nude mice (Ceaglio et al., 2010a). The same was observed for both pegylated forms of rhIFN-α2 (PEG-Intron and PEGASYS), whose dramatic activity reduction was compensated by their enhanced *in vivo* activity due to their prolonged duration of action (Pedder, 2003). Regarding other proteins different from IFNs, a long-acting rhGH variant was developed by XTEN technology$^{TM}$, which consists in the fusion of an unstructured hydrophilic sequence of 864 amino acids to the protein of interest (Cleland et al., 2012). Although *in vitro* potency of this chimera was reduced 12-fold compared to native rhGH, *in vivo* potency was increased because of the prolonged exposure to the target tissues and organs. Remarkably, this was a direct consequence of its lower affinity for the hGH receptor, which minimized the receptor-mediated clearance. For therapeutic recombinant proteins, the reduction of the binding affinity for their receptor would also contribute to lessen their side-effects, with prevalence of their expected actions (Cleland et al., 2012).

Regarding pharmacokinetics of the IFN variants, the wild-type cytokine was rapidly absorbed and cleared while CTP-IFN and IFN-CTP showed a fast distribution phase followed by a slower elimination one. Contrarily, both phases of the CTP-IFN-CTP pharmacokinetics were markedly prolonged. These results were consistent with previous studies in which hCG β-subunit-derived CTP region was fused to different proteins with the aim of retaining them in plasma circulation for a longer period of time and reducing their plasma elimination. For example, the $t_{1/2}$ of FSH was doubled by fusing one CTP sequence between α- and β-subunit of the hormone (Klein et al., 2003). Similar results were obtained for other molecules such as GH and EPO. Variants of hGH containing three units of CTP region exhibited a 5-fold increment in $t_{1/2}$ (Fares et al., 2010) and variants of rhEPO with the same amount of CTP repeats achieved a 3-fold increment in the same parameter (Fares et al., 2011). As it has been reported by (Lee et al., 2006), the higher $t_{1/2}$ values conferred by the stabilizing effect of CTP may be a consequence of both the structure of the peptide itself and the *O*-glycan content. Nevertheless, the same authors demonstrated a lower *in vivo* effect of mutated CTP without glycosylation sites. These findings show the importance of *O*-glycosylation for reaching the maximum potential of this strategy in order to improve protein's efficacy. Also, the results showed in our work can be correlated with what we have previously found through the addition of *N*-glycans, *i.e.*, that the successive addition of *N*-linked carbohydrates lengthens both the absorption–distribution and the elimination pharmacokinetic phases (Ceaglio et al., 2008). In this case, increasing the content of *O*-linked glycans from one (in wild-type IFN) to four (in CTP-IFN and IFN-CTP) and up to eight (in CTP-IFN-CTP), as determined *in silico*, results in the same effect, with notable increases in $t_{1/2}$ and decreases in $CL_{app}$. Relationships between pharmacokinetic properties and sialic acid content of the three molecules (wild-type IFN, CTP-IFN-CTP and 4N-IFN) may support the idea that this residue constitutes a determining factor which contributes to delay protein's clearance by several mechanisms, including reduction of glomerular filtration by charge-repulsion, restriction of

binding to hepatic asialoglycoprotein receptors and decrease of receptor-mediated endocytosis (Bork et al., 2009; Koury, 2003; Morell et al., 1971).

One of the main challenges of the development of therapeutic proteins is to achieve their chemical and physical stability through time. Our results showed that increasing the content of O-glycans protects rhIFN-α2b from high temperature inactivation. However, a single O-glycosylation site does not seem to be enough for improving thermal stability of the cytokine, since no significant differences were found between the behavior of non-glycosylated and wild-type IFN. The addition of two CTP moieties increased the number of potential O-glycosylation sites to nine, and this larger content of attached carbohydrate chains might account for the stabilization of the conformation of the CTP-IFN-CTP variant. We have shown that the addition of four potential N-glycosylation sites in 4N-IFN also results in an increased heat resistance, preserving more than 65% of residual activity after incubation at 95 °C (Ceaglio et al., 2010b), indicating a general effect of stabilization of both O- and N-linked oligosaccharide chains towards this denaturing agent. Additionally, these findings are in accordance with other studies which have demonstrated the benefits of glycosylation in other therapeutic proteins in terms of improved stability (Durocher and Butler, 2009). For example, mammalian cells-derived erythropoietin containing N- and O-linked carbohydrates exhibited improved conformational stability against chemical denaturing agents, pH and temperature when compared to the hormone expressed in E. coli (Narhi et al., 1991). Nonetheless, as the stabilizing effect of glycosylation has demonstrated to be highly protein-dependent (Wang, 1999), the favorable effect of CTP on the thermal stability of rhIFN-α2b is worthy to be highlighted, since stability is critical for both efficacy and safety of protein-based therapeutics.

The addition of O-glycans also increased the stability of CTP-IFN-CTP in the presence of human serum, probably by masking protease cleavage sites, generating, for example, steric hindrance which blocks enzymatic activity. This higher resistance to plasma protease inactivation might result in a positive effect on the cytokineís pharmacokinetics in humans, contributing to prolong its in vivo half-life and thus, to enhance its in vivo activity. Indeed, there are many examples of therapeutically relevant proteins whose proteolytic degradation has been decreased by introducing new glycosyl moieties or just by their natural glycans (Sola and Griebenow, 2010). N-glycan's protection against rat plasma inactivation was also demonstrated for 4N-IFN and could be successful translated into a beneficial effect on the cytokineís pharmacokinetics in that animal model (Ceaglio et al., 2010b). The importance of carbohydrates on glycosylated human granulocyte colony stimulating factor in protecting against serum inactivation was also described, since serum rapidly reduced the biological activity of the non-glycosylated protein (Carter et al., 2004). Also, glycosylation of a cytotoxic amphibian ribonuclease (ranpirnase, onconase™) increased both its Tm and its resistance to proteinase K, suggesting that its higher conformational stability resulted in the greatly improved toxicity against cancer cells (Kim et al., 2004).

Glycosylation studies indicated the presence of the two most common O-glycan core structures (core 1 and core 2) in CTP-IFN-CTP. Mono- and bisialylated core 1 glycans seemed to be the most important structures, with a small contribution of mono- and bisialylated core 2 structures. On the one hand, different authors agree that bisialylated core 1 structures are the major components of the O-glycans attached to Thr106 both in wild-type hIFN-α2b (Adolf et al., 1991) and in 4N-IFN (Ceaglio et al., 2010a). On the other hand, it has been well described the existence of two natural occurring variants of hCG whose structural difference strictly lies in their carbohydrate structure. Significant and consistent differences have been found between the four O-linked oligosaccharides on β-subunit, that is to say, the ones attached to CTP: while a trisac-charide corresponding to monosialylated core 1 is the principal structure found in pregnancy hCG, an hexasaccharide consisting of bisialylated core 2 constitutes the highest percentage of glycans encountered in hyperglycosylated hCG from choriocarcinoma patients (Cole, 2010; Cole and Khanlian, 2007). Less is known about the four O-glycans in rhCG produced in CHO cells, but our results indicate that O-glycans derived from CTP-IFN-CTP resemble more the glycan structures found in normal cells rather than in transformed ones.

In conclusion, the long-lasting properties of CTP were once more demonstrated using IFN as a model protein while a novel feature depending on the O-glycans was described. Fusing CTP to the N- and C-terminal ends of rhIFN-α2b showed the influence of O-glycans on thermal stress and plasma protease inactivation and allowed to relate their effects with the structural stability and pharmacokinetics of CTP-fused IFN. Therefore, CTP has shown to be a stabilizing tag to successfully modify rhIFN-α2b properties by O-glycosylation, which in turn can promote the increase in its in vivo biological activity.

## Conflict of interest

The authors declare that they have no conflict of interests.

## Author contributions

N.C and M.O. designed experiments; A.G., M.B.T. and D.C. performed the experiments; R.K., M.E., N.C. and M.O. supervised the research, N.C. wrote the manuscript, M.O. and R.K. revised the manuscript. All authors approve the final article.

## Acknowledgements

## References

Adolf, G.R., Kalsner, I., Ahorn, H., Maurer-Fogy, I., Cantell, K., 1991. Natural human interferon-alpha 2 is O-glycosylated. Biochem. J. 276 (Pt. 2), 511–518.

Bai, X., Li, D., Zhu, J., Guan, Y., Zhang, Q., Chi, L., 2015. From individual proteins to proteomic samples: characterization of O-glycosylation sites in human chorionic gonadotropin and human-plasma proteins. Anal. Bioanal. Chem. 407, 1857–1869.

Baker, D.E., 2001. Pegylated interferons. Rev. Gastroenterol. Disord. 1, 87–99.

Birken, S., Canfield, R.E., 1977. Isolation and amino acid sequence of COOH-terminal fragments from the beta subunit of human choriogonadotropin. J. Biol. Chem. 252, 5386–5392.

Bocci, V., Carraro, F., Naldini, A., Cagol, P.P., Pasqual, E.M., Prevaldi, C., Casara, D., 1990. Distribution of human recombinant interferon-alpha 2 in rat plasma, liver, and experimental liver metastases. Mol. Biother. 2, 233–234.

Borden, E.C., Sen, G.C., Uze, G., Silverman, R.H., Ransohoff, R.M., Foster, G.R., Stark, G.R., 2007. Interferons at age 50: past, current and future impact on biomedicine. Nat. Rev. Drug Discov. 6, 975–990.

Bork, K., Horstkorte, R., Weidemann, W., 2009. Increasing the sialylation of therapeutic glycoproteins: the potential of the sialic acid biosynthetic pathway. J. Pharm. Sci. 98, 3499–3508.

Carter, C.R., Keeble, J.R., Thorpe, R., 2004. Human serum inactivates non-glycosylated but not glycosylated granulocyte colony stimulating factor

by a protease dependent mechanism: significance of carbohydrates on the glycosylated molecule. Biologicals 32, 37–47.

Ceaglio, N., Etcheverrigaray, M., Conradt, H.S., Grammel, N., Kratje, R., Oggero, M., 2010a. Highly glycosylated human alpha interferon: an insight into a new therapeutic candidate. J. Biotechnol. 146, 74–83.

Ceaglio, N., Etcheverrigaray, M., Kratje, R., Oggero, M., 2010b. Influence of carbohydrates on the stability and structure of a hyperglycosylated human interferon alpha mutein. Biochimie 92, 971–978.

Ceaglio, N., Etcheverrigaray, M., Kratje, R., Oggero, M., 2008. Novel long-lasting interferon alpha derivatives designed by glycoengineering. Biochimie 90, 437–449.

Cleland, J.L., Geething, N.C., Moore, J.A., Rogers, B.C., Spink, B.J., Wang, C.W., Alters, S.E., Stemmer, W.P., Schellenberger, V., 2012. A novel long-acting human growth hormone fusion protein (VRS-317): enhanced in vivo potency and half-life. J. Pharm. Sci. 101, 2744–2754.

Cole, L.A., 2010. Hyperglycosylated hCG, a review. Placenta 31, 653–664.

Cole, L.A., Khanlian, S.A., 2007. Hyperglycosylated hCG: a variant with separate biological functions to regular hCG. Mol. Cell Endocrinol. 260–262, 228–236.

Choi, S.H., Park, T.G., 2006. G-CSF loaded biodegradable PLGA nanoparticles prepared by a single oil-in-water emulsion method. Int. J. Pharm. 311, 223–228.

de Weerd, N.A., Samarajiwa, S.A., Hertzog, P.J., 2007. Type I interferon receptors: biochemistry and biological functions. J. Biol. Chem. 282, 20053–20057.

Depetris, M., Casalis, P., Kratje, R., Etcheverrigaray, M., Oggero, M., 2008. A scFv antibody fragment as a therapeutic candidate to neutralize a broad diversity of human IFN-alpha subtypes. J. Immunol. Methods 334, 104–113.

Dull, T., Zufferey, R., Kelly, M., Mandel, R.J., Nguyen, M., Trono, D., Naldini, L., 1998. A third-generation lentivirus vector with a conditional packaging system. J. Virol. 72, 8463–8471.

Durocher, Y., Butler, M., 2009. Expression systems for therapeutic glycoprotein production. Curr. Opin. Biotechnol. 20, 700–707.

Egrie, J.C., Dwyer, E., Browne, J., Hitz, A., Lykos, M.A., 2003. Darbepoetin alfa has a longer circulating half-life and greater in vivo potency than recombinant human erythropoietin. Exp. Hematol. 31, 290–299.

El-Baky, N.A., Redwan, E.M., 2015. Therapeutic alpha-interferons protein: structure, production, and biosimilar. Prep. Biochem. Biotechnol. 45, 109–127.

Elliott, S., Lorenzini, T., Asher, S., Aoki, K., Brankow, D., Buck, L., Busse, L., Chang, D., Fuller, J., Grant, J., Hernday, N., Hokum, M., Hu, S., Knudten, A., Levin, N., Komorowski, R., Martin, F., Navarro, R., Osslund, T., Rogers, G., Rogers, N., Trail, G., Egrie, J., 2003. Enhancement of therapeutic protein in vivo activities through glycoengineering. Nat. Biotechnol. 21, 414–421.

EMA/65507/2013, rev 1. BEMFOLA. Assessment report. European Medicine Agency. Committee for Medicinal Products for Human Use (CHMP), EMEA, 2013. [Cited June 2014], available from: http://www.ema.europa.eu/docs/en_GB/document_library/EPAR_-_Public_assessment_report/human/002615/WC500166820.pdf.

Familletti, P.C., Rubinstein, S., Pestka, S., 1981. A convenient and rapid cytopathic effect inhibition assay for interferon. Methods Enzymol. 78, 387–394.

Fares, F., Ganem, S., Hajouj, T., Agai, E., 2007. Development of a long-acting erythropoietin by fusing the carboxyl-terminal peptide of human chorionic gonadotropin beta-subunit to the coding sequence of human erythropoietin. Endocrinology 148, 5081–5087.

Fares, F., Guy, R., Bar-Ilan, A., Felikman, Y., Fima, E., 2010. Designing a long-acting human growth hormone (hGH) by fusing the carboxyl-terminal peptide of human chorionic gonadotropin beta-subunit to the coding sequence of hGH. Endocrinology 151, 4410–4417.

Fares, F., Havron, A., Fima, E., 2011. Designing a long acting erythropoietin by fusing three carboxyl-terminal peptides of human chorionic gonadotropin beta subunit to the N-terminal and C-terminal coding sequence. Int. J. Cell Bio. 2011, 275063.

Fares, F.A., Suganuma, N., Nishimori, K., LaPolt, P.S., Hsueh, A.J., Boime, I., 1992. Design of a long-acting follitropin agonist by fusing the C-terminal sequence of the chorionic gonadotropin beta subunit to the follitropin beta subunit. Proc. Natl. Acad. Sci. U. S. A. 89, 4304–4308.

Furuhashi, M., Shikone, T., Fares, F.A., Sugahara, T., Hsueh, A.J., Boime, I., 1995. Fusing the carboxy-terminal peptide of the chorionic gonadotropin (CG) beta-subunit to the common alpha-subunit: retention of O-linked glycosylation and enhanced in vivo bioactivity of chimeric human CG. Mol. Endocrinol. 9, 54–63.

Ghaderi, D., Taylor, R.E., Padler-Karavani, V., Diaz, S., Varki, A., 2010. Implications of the presence of N-glycolylneuraminic acid in recombinant therapeutic glycoproteins. Nat. Biotechnol. 28, 863–867.

Ghaderi, D., Zhang, M., Hurtado-Ziola, N., Varki, A., 2012. Production platforms for biotherapeutic glycoproteins occurrence, impact, and challenges of non-human sialylation. Biotechnol. Genet. Eng. Rev. 28, 147–175.

Isaacs, A., Lindenmann, J., 1957. Virus interference. I. The interferon. Proc. R. Soc. Lond. B Biol. Sci. 147, 258–267.

Jaks, E., Gavutis, M., Uze, G., Martal, J., Piehler, J., 2007. Differential receptor subunit affinities of type I interferons govern differential signal activation. J. Mol. Biol. 366, 525–539.

Jensen, P.H., Kolarich, D., Packer, N.H., 2010. Mucin-type O-glycosylation—putting the pieces together. FEBS J. 277, 81–94.

Joshi, L., Murata, Y., Wondisford, F.E., Szkudlinski, M.W., Desai, R., Weintraub, B.D., 1995. Recombinant thyrotropin containing a beta-subunit chimera with the human chorionic gonadotropin-beta carboxy-terminus is biologically active, with a prolonged plasma half-life: role of carbohydrate in bioactivity and metabolic clearance. Endocrinology 136, 3839–3848.

Kalie, E., Jaitin, D.A., Abramovich, R., Schreiber, G., 2007. An interferon alpha2 mutant optimized by phage display for IFNAR1 binding confers specifically enhanced antitumor activities. J. Biol. Chem. 282, 11602–11611.

Kalie, E., Jaitin, D.A., Podoplelova, Y., Piehler, J., Schreiber, G., 2008. The stability of the ternary interferon-receptor complex rather than the affinity to the individual subunits dictates differential biological activities. J. Biol. Chem. 283, 32925–32936.

Kim, B.M., Kim, H., Raines, R.T., Lee, Y., 2004. Glycosylation of onconase increases its conformational stability and toxicity for cancer cells. Biochem. Biophys. Res. Commun. 315, 976–983.

Klein, J., Lobel, L., Pollak, S., Lustbader, B., Ogden, R.T., Sauer, M.V., Lustbader, J.W., 2003. Development and characterization of a long-acting recombinant hFSH agonist. Hum. Reprod. 18, 50–56.

Kong, Y., Joshi, H.J., Schjoldager, K.T., Madsen, T.D., Gerken, T.A., Vester-Christensen, M.B., Wandall, H.H., Bennett, E.P., Levery, S.B., Vakhrushev, S.Y., Clausen, H., 2015. Probing polypeptide GalNAc-transferase isoform substrate specificities by in vitro analysis. Glycobiology 25, 55–65.

Kontsek, P., 1994. Human type I interferons: structure and function. Acta Virol. 38, 345–360.

Koury, M.J., 2003. Sugar coating extends half-lives and improves effectiveness of cytokine hormones. Trends Biotechnol. 21, 462–464.

Kozak, R.P., Royle, L., Gardner, R.A., Fernandes, D.L., Wuhrer, M., 2012. Suppression of peeling during the release of O-glycans by hydrazinolysis. Anal. Biochem. 423, 119–128.

Leader, B., Baca, Q.J., Golan, D.E., 2008. Protein therapeutics: a summary and pharmacological classification. Nat. Rev. Drug Discov. 7, 21–39.

Lee, D.E., Son, W., Ha, B.J., Oh, M.S., Yoo, O.J., 2006. The prolonged half-lives of new erythropoietin derivatives via peptide addition. Biochem. Biophys. Res. Commun. 339, 380–385.

Leung, M.-Y., Cardenas, G.A., Almeida, I.C., Gerken, T.A., 2014 Isoform Specific O-Glycosylation Prediction (ISOGlyP) Version 1.2., p. Available at http://isoglyp.utep.edu (accessed 31.10.14.).

Lin, F.C., Young, H.A., 2014. Interferons: success in anti-viral immunotherapy. Cytokine Growth Factor Rev. 25, 369–376.

Mahmood, I., Green, M.D., 2005. Pharmacokinetic and pharmacodynamic considerations in the development of therapeutic proteins. Clin. Pharmacokinet. 44, 331–347.

Markert, Y., Koditz, J., Mansfeld, J., Arnold, U., Ulbrich-Hofmann, R., 2001. Increased proteolytic resistance of ribonuclease A by protein engineering. Protein Eng. 14, 791–796.

Marshall, S.A., Lazar, G.A., Chirino, A.J., Desjarlais, J.R., 2003. Rational design and engineering of therapeutic proteins. Drug Discov. Today 8, 212–221.

Matzuk, M.M., Hsueh, A.J., Lapolt, P., Tsafriri, A., Keene, J.L., Boime, I., 1990. The biological role of the carboxyl-terminal extension of human chorionic gonadotropin [corrected] beta-subunit. Endocrinology 126, 376–383.

Morell, A.G., Gregoriadis, G., Scheinberg, I.H., Hickman, J., Ashwell, G., 1971. The role of sialic acid in determining the survival of glycoproteins in the circulation. J. Biol. Chem. 246, 1461–1467.

Naldini, L., Blomer, U., Gallay, P., Ory, D., Mulligan, R., Gage, F.H., Verma, I.M., Trono, D., 1996. In vivo gene delivery and stable transduction of nondividing cells by a lentiviral vector. Science 272, 263–267.

Narhi, L.O., Arakawa, T., Aoki, K.H., Elmore, R., Rohde, M.F., Boone, T., Strickland, T.W., 1991. The effect of carbohydrate on the structure and stability of erythropoietin. J. Biol. Chem. 266, 23022–23026.

Nederman, T., Karlstrom, E., Sjodin, L., 1990. An in vitro bioassay for quantitation of human interferons by measurements of antiproliferative activity on a continuous human lymphoma cell line. Biologicals 18, 29–34.

Noguchi, A., Mukuria, C.J., Suzuki, E., Naiki, M., 1995. Immunogenicity of N-glycolylneuraminic acid-containing carbohydrate chains of recombinant human erythropoietin expressed in Chinese hamster ovary cells. J. Biochem. 117, 59–62.

O'Kelly, P., Thomsen, L., Tilles, J.G., Cesario, T., 1985. Inactivation of interferon by serum and synovial fluids. Proc. Soc. Exp. Biol. Med. 178, 407–411.

Paul, F., Pellegrini, S., Uze, G., 2015. IFNA2: the prototypic human alpha interferon. Gene 567, 132–137.

Pedder, S.C., 2003. Pegylation of interferon alfa: structural and pharmacokinetic properties. Semin. Liver Dis. 23 (Suppl. 1), 19–22.

Peleg-Shulman, T., Tsubery, H., Mironchik, M., Fridkin, M., Schreiber, G., Shechter, Y., 2004. Reversible PEGylation: a novel technology to release native interferon alpha2 over a prolonged time period. J. Med. Chem. 47, 4897–4904.

Petersen, T.N., Brunak, S., von Heijne, G., Nielsen, H., 2011. SignalP 4.0: discriminating signal peptides from transmembrane regions. Nat. Methods 8, 785–786.

Pierce, J.G., Parsons, T.F., 1981. Glycoprotein hormones: structure and function. Annu. Rev. Biochem. 50, 465–495.

Podobnik, B., Helk, B., Smilovic, V., Skrajnar, S., Fidler, K., Jevsevar, S., Godwin, A., Williams, P., 2015. Conjugation of PolyPEG to interferon alpha extends serum half-life while maintaining low viscosity of the conjugate. Bioconjugate Chem. 26, 452–459.

Roberts, M.J., Bentley, M.D., Harris, J.M., 2002. Chemistry for peptide and protein PEGylation. Adv. Drug Deliv. Rev. 54, 459–476.

Royle, L., Mattu, T.S., Hart, E., Langridge, J.I., Merry, A.H., Murphy, N., Harvey, D.J., Dwek, R.A., Rudd, P.M., 2002. An analytical and structural database provides a strategy for sequencing O-glycans from microgram quantities of glycoproteins. Anal. Biochem. 304, 70–90.

Rudd, P.M., Dwek, R.A., 1997. Glycosylation: heterogeneity and the 3D structure of proteins. Crit. Rev. Biochem. Mol. Biol. 32, 1–100.

Samoudi, M., Tabandeh, F., Minuchehr, Z., Ahangari Cohan, R., Nouri Inanlou, D., Khodabandeh, M., Sabery Anvar, M., 2015. Rational design of hyper-glycosylated interferon beta analogs: a computational strategy for glycoengineering. J. Mol. Graph Model 56, 31–42.

Shargel, L., Wu-Pong, S., Yu, A.B.C., 2005. Applied Biopharmaceutics & Pharmacokinetics. Appleton & Lange Reviews/McGraw-Hill, Medical Pub. Division, New York.

Sinclair, A.M., Elliott, S., 2005. Glycoengineering: the effect of glycosylation on the properties of therapeutic proteins. J. Pharm. Sci. 94, 1626–1635.

Sleijfer, S., Bannink, M., Van Gool, A.R., Kruit, W.H., Stoter, G., 2005. Side effects of interferon-alpha therapy. Pharm. World Sci. 27, 423–431.

Sola, R.J., Griebenow, K., 2010. Glycosylation of therapeutic proteins: an effective strategy to optimize efficacy. BioDrugs 24, 9–21.

Steentoft, C., Vakhrushev, S.Y., Joshi, H.J., Kong, Y., Vester-Christensen, M.B., Schjoldager, K.T., Lavrsen, K., Dabelsteen, S., Pedersen, N.B., Marcos-Silva, L., Gupta, R., Bennett, E.P., Mandel, U., Brunak, S., Wandall, H.H., Levery, S.B., Clausen, H., 2013. Precision mapping of the human O-GalNAc glycoproteome through SimpleCell technology. EMBO J. 32, 1478–1488.

Subramanian, G.M., Fiscella, M., Lamouse-Smith, A., Zeuzem, S., McHutchison, J.G., 2007. Albinterferon alpha-2b: a genetic fusion protein for the treatment of chronic hepatitis C. Nat. Biotechnol. 25, 1411–1419.

Thomas, C., Moraga, I., Levin, D., Krutzik, P.O., Podoplelova, Y., Trejo, A., Lee, C., Yarden, G., Vleck, S.E., Glenn, J.S., Nolan, G.P., Piehler, J., Schreiber, G., Garcia, K.C., 2011. Structural linkage between ligand discrimination and receptor activation by type I interferons. Cell 146, 621–632.

Uze, G., Tavernier, J., 2015. High efficiency targeting of IFN-alpha activity: possible applications in fighting tumours and infections. Cytokine Growth Factor Rev. 26, 179–182.

Van den Steen, P., Rudd, P.M., Dwek, R.A., Opdenakker, G., 1998. Concepts and principles of O-linked glycosylation. Crit. Rev. Biochem. Mol. Biol. 33, 151–208.

Wang, W., 1999. Instability, stabilization, and formulation of liquid protein pharmaceuticals. Int. J. Pharm. 185, 129–188.

Wopereis, S., Abd Hamid, U.M., Critchley, A., Royle, L., Dwek, R.A., Morava, E., Leroy, J.G., Wilcken, B., Lagerwerf, A.J., Huijben, K.M., Lefeber, D.J., Rudd, P.M., Wevers, R.A., 2006. Abnormal glycosylation with hypersialylated O-glycans in patients with Sialuria. Biochim. Biophys. Acta 1762, 598–607.

Yuan, L., Wang, J., Shen, W.C., 2008. Lipidization of human interferon-alpha: a new approach toward improving the delivery of protein drugs. J. Control Release 129, 11–17.